C_2-Symmetric Ni(II) α-Diimines Featuring Cumyl-Derived Ligands: Synthesis of Improved Elastomeric Regioblock Polypropylenes

Jeffrey M. Rose,[†] Fanny Deplace,[‡] Nathaniel A. Lynd,[‡] Zhigang Wang,[‡] Atsushi Hotta,[‡] Emil B. Lobkovsky,[†] Edward J. Kramer,[‡] and Geoffrey W. Coates*[,†]

Department of Chemistry and Chemical Biology, Baker Laboratory, Cornell University, Ithaca, New York 14853, and Mitsubishi Chemical Center for Advanced Materials and the Departments of Materials and Chemical Engineering, University of California, Santa Barbara, California 93106

Received September 2, 2008

ABSTRACT: A series of chiral, nickel α-diimine complexes featuring ligands based on bulky cumyl-substituted aniline moieties was synthesized. Each complex was capable of polymerizing propylene upon activation with methylaluminoxane (MAO). The catalysts were shown to be highly regioregular and isoselective for propylene polymerization at low temperature (e.g., −60 °C), whereas at higher reaction temperatures (e.g., 0 °C) the catalysts furnished regioirregular polypropylene (rirPP) composed of 1,2- and 3,1-enchainments. Many of the catalysts exhibited living behavior for propylene polymerization from −78 to 0 °C. From the screening results, the best catalyst was selected and used to produce regioblock polypropylenes featuring three or five blocks. Mechanical testing revealed that the materials exhibited good elastomeric behavior and improved performance at elevated temperatures (e.g., 65 °C) over block copolymers synthesized using a previously prepared chiral, nickel α-diimine catalyst.

Introduction

Attaining polymeric materials with desirable physical properties hinges on the ability to control both polymer structure and molecular weight. Stereo- and regioselective catalysts that exhibit living behavior have emerged from decades of research.[1] In particular, many important developments for late metal-catalyzed olefin polymerization have been reported during the last 15 years. Rivaling well-established early metal olefin polymerization catalysts, there now exist a number of late metal catalysts that exhibit high polymerization activities,[2,3] stereoselectivity,[4−6] and living behavior.[6−13] In addition, late metal catalysts enable the development of polymeric materials not attainable from early metal catalysts. The ability to incorporate functional comonomers into polyolefins[2,14−19] and the ability to harness chain-walking[2,13,20,21] to attain novel polymeric structures are notable facets of late metal catalysts.

We have previously reported a chiral Ni(II) α-diimine complex[6] (*rac*-**1**, Scheme 1) which, upon activation, polymerizes ethylene,[22] propylene,[6] and higher α-olefins[13] in a living fashion. The catalyst is highly isoselective for propylene polymerization at low temperature (e.g., −60 °C) and exhibits temperature-dependent regioselectivity whereby at low reaction temperatures the catalyst furnishes 1,2-enchained, isotactic polypropylene (iPP) and higher reaction temperatures (e.g., 0 °C) furnish regioirregular polypropylene (rirPP) composed of 1,2- and 3,1-enchainments. We have exploited this interesting trend in selectivity to synthesize elastomeric regioblock copolymers featuring three and five blocks.[23] This was accomplished by varying reaction temperature throughout the course of polymerization giving rise to either semicrystalline, isotactic polypropylene or amorphous, regioirregular blocks. The catalyst also exhibits interesting behavior for higher α-olefin polymerization.[13] Through controlled chain-walking, *rac*-**1**/methylaluminoxane (*rac*-**1**/MAO) can give rise to predominantly *ω*,2-enchained poly(α-olefin)s whereby a C_n linear α-olefin is polymerized to form a polymer with a repeat unit $[-CH(CH_3)(CH_2)_{n-2}-]$ (Scheme 1).

Scheme 1. Olefin Polymerization Behavior of *rac*-1/MAO

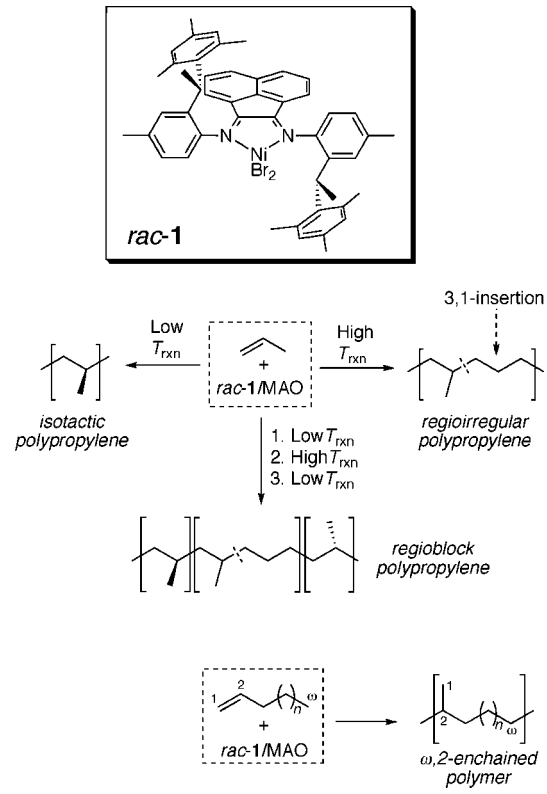

Although *rac*-**1**/MAO exhibits unique and desirable olefin polymerization behavior, the catalyst has deficiencies which we have sought to address. Specifically, the catalyst exhibits very low activities for propylene polymerization at low temperatures (at −78 °C, polymerization proceeds with a turnover frequency (TOF) of 1 h^{-1}). Further, although the iso- and regioselectivities of the catalyst are quite good for propylene polymerization at low temperature, the melting point of the resultant polymer is 137 °C which is significantly lower than that expected for isotactic polypropylene (165 °C). It is believed that incorporation

* Corresponding author. E-mail: gc39@cornell.edu.
[†] Cornell University.
[‡] University of California.

10.1021/ma8019943 CCC: $40.75
Published on Web 11/26/2008

of higher melting isotactic polypropylene blocks into the aforementioned regioblock copolymers could yield materials with improved elastomeric behavior. In addition, an increase in catalyst activity could greatly decrease the time necessary to synthesize these regioblock copolymers. Herein we report a series of new chiral Ni(II) α-diimine catalysts that show improved activities and iso- and regioselectivities for propylene polymerization.

Experimental Section

Synthesis of Complexes *rac*-1−*rac*-7. See the Supporting Information.

General Procedures. All manipulations of air- and/or water-sensitive compounds were carried out under dry nitrogen using a Braun UniLab drybox or standard Schlenk techniques. Toluene was purified over columns of alumina and copper (Q5). Methylene chloride was purified over an alumina column and degassed by three freeze−pump−thaw cycles before use. Propylene (Matheson, ultrahigh purity) was purified over columns of Selexorb COS alumina donated by Coastal Chemical Company, and copper Q5 purchased from Engelhard Corporation. MMAO-7 (7.1 wt % Al in Isopar E, Akzo Nobel) was used as received. PMAO-IP (13 wt % Al in toluene, Akzo Nobel) was dried in vacuo to remove residual trimethylaluminum and used as a solid white powder.

Polymer Characterization. ^{1}H and ^{13}C NMR spectra of the polymers were recorded on a Varian Inova spectrometer (500 MHz) equipped with a ^{1}H/BB switchable with *Z*-pulse field gradient probe and referenced versus residual nondeuterated solvent shifts. The polymer samples were dissolved in 1,1,2,2-tetrachloroethane-d_2 in a 5 mm o.d. tube, and spectra were collected at 135 °C. Molecular weights (M_n and M_w) and polydispersities (M_w/M_n) were determined by high-temperature gel permeation chromatography (GPC), using a Waters Alliance GPCV 2000 GPC equipped with a Waters DRI detector and viscometer. The column set (four Waters HT 6E and one Waters HT 2) was eluted with 1,2,4-trichlorobenzene containing 0.01 wt % di-*tert*-butyl-hydroxytoluene (BHT) at 1.0 mL/min at 140 °C. Data were calibrated using monomodal polyethylene standards (from Polymer Standards Service). Polymers were placed in a 140 °C oven for 24 h prior to molecular weight measurements.

Differential scanning calorimetry (DSC) was performed using a TA Instruments Q1000 calorimeter equipped with an automated sampler. Analyses were performed in crimped aluminum pans under nitrogen, and data were collected from the second heating run at a heating rate of 10 °C/min from −100 to 200 °C and processed with the TA Q series software.

Propylene Polymerizations, General Procedure (Tables 1−3). In a glovebox, toluene and a solution of MMAO-7 (1.91 M in Isopar E) was added to a 6 ounce (180 mL) round-bottom Laboratory Crest reaction vessel (Andrews Glass). The vessel was cooled to −78 °C, and the appropriate mass of propylene was condensed in. The reaction mixture was then allowed to equilibrate at the desired temperature for 10 min upon which the appropriate complex was injected as a solution in 2 mL of dry, degassed CH_2Cl_2. The polymerization was quenched with methanol, the reaction mixture was precipitated into a copious amount of acidic methanol (2% HCl(aq)), and the resulting suspension was allowed to stir overnight. The polymer was isolated, rinsed with methanol, and dried to constant weight in vacuo at 60 °C.

Block Copolymer Synthesis Using *rac*-1. For ***isoTB*** and ***isoPB*** see the previous report.[23]

Block Copolymer Synthesis Using *rac*-7, General Procedure (Table 4). In a glovebox, a given volume of toluene and PMAO-IP were added to a 6 ounce (180 mL) round-bottom Laboratory Crest reaction vessel (Andrews Glass). The vessel was cooled to −78 °C, and a given mass of propylene was condensed in at 30 psig. The reaction mixture was then allowed to equilibrate at −60 °C for 10 min upon which a given amount of *rac*-**7** was injected as a solution in 2 mL of dry, degassed CH_2Cl_2. After time t_1 an aliquot was taken from the reaction mixture via canula using an overpressure of 30 psig propylene. The reactor was then transferred to a 0 °C bath and allowed to react for time t_2. At this point, the reactor was transferred back to the −60 °C bath, and when the pressure within the reactor was approximately 20 psig a second aliquot was taken via canula using an overpressure of 30 psig propylene. The third block was allowed to form over time t_3. At this point, for triblock copolymers, the reaction was quenched with methanol. For the pentablock copolymer two subsequent blocks were added at 0 and −60 °C over times t_4 and t_5, respectively, before quenching. In all cases quenching was followed by precipitation of the reaction mixture into a copious amount of acidic methanol (2% HCl(aq)), and allowing the resulting suspension to stir overnight. The polymer was isolated, rinsed with methanol, and dried to constant weight in vacuo at 60 °C. The samples were purified by dissolving each in hot toluene and then filtering the resulting solution though a glass frit layered with Celite, alumina, and silica. To the filtrate was added 0.01 wt % BHT, the toluene was removed in vacuo, and the polymer was dried in vacuo at 60 °C to constant weight.

isoTB2. This was synthesized using the general block copolymer synthesis procedure: 20 μmol of *rac*-**7**, 30 mL of toluene, three blocks formed over times t_1 = 7.5 h, t_2 = 35 min, and t_3 = 16 h at −60, 0, and −60 °C, respectively; yield = 2.15 g.

isoTB3. This was synthesized using the general block copolymer synthesis procedure: 15 μmol of *rac*-**7**, 50 mL of toluene, three blocks formed over times t_1 = 7.5 h, t_2 = 60 min, and t_3 = 16 h at −60, 0, and −60 °C, respectively; yield = 2.11 g.

isoTB4. This was synthesized using the general block copolymer synthesis procedure: 12 μmol of *rac*-**7**, 50 mL of toluene, three blocks formed over times t_1 = 7.5 h, t_2 = 90 min, and t_3 = 16 h at −60, 0, and −60 °C, respectively; yield = 1.83 g.

isoPB2. This was synthesized using the general block copolymer synthesis procedure: 11 μmol of *rac*-**7**, 75 mL of toluene, five blocks formed over times t_1 = 7 h, t_2 = 60 min, t_3 = 16 h, t_4 = 100 min, and t_5 = 24 h at −60, 0, −60, 0, and −60 °C, respectively; yield = 1.84 g.

Tensile Mechanical Testing. Samples synthesized using *rac*-**7**/MAO were melt-pressed into films at 200 °C followed by slow cooling to room temperature. The films were cut into dog bone shaped samples with a thickness of about 0.5 mm, a length of 7.5 mm, and a width of 2 mm.

Cut samples were then either stretched to fracture or up to a given tensile strain using an Instron 1123 testing machine. Tensile experiments were performed at room temperature (∼20 °C) and at 65 °C. The crosshead velocity was set equal to 5.08 mm·min^{-1} corresponding to an initial strain rate of about 0.01 s^{-1}. Two types of mechanical tests were performed as follows: (1) samples were stretched monotonically to fracture, and stress−strain curves were recorded. True stresses were computed by correcting measured nominal stress values for the specimen area decrease at large tensile strains; (2) step cycle tests were performed that combine a stepwise stretching of the tensile specimen with unloading−reloading cycles. In each step, the sample was extended step by step up to different strains. Once the sample reached the appropriate strain, the crosshead direction was reversed and the sample strain was decreased at the same crosshead velocity until zero stress was achieved. The sample was then extended again at the same constant crosshead speed until it reached the next targeted step-strain. The step cycle test was performed until the sample fractured or in some cases until the sample pulled from the grips. With this step cycle test, we measured the elastic recovery of the materials. The elastic recovery (%) is defined as the strain recovered upon unloading divided by the maximum strain reached during that step.

Discussion

Complex Synthesis. A noteworthy feature of *rac*-**1** is that it contains two stereocenters as its ancillary ligand is based on a chiral aniline derivative. We have previously reported a synthetic route to such anilines whereby acid-catalyzed ortho-alkylation of a para-substituted aniline derivative with a substituted styrene yields a mono- or disubstituted product.[24] Our strategy for

Scheme 2. General Synthetic Routes to *rac*-2−*rac*-7

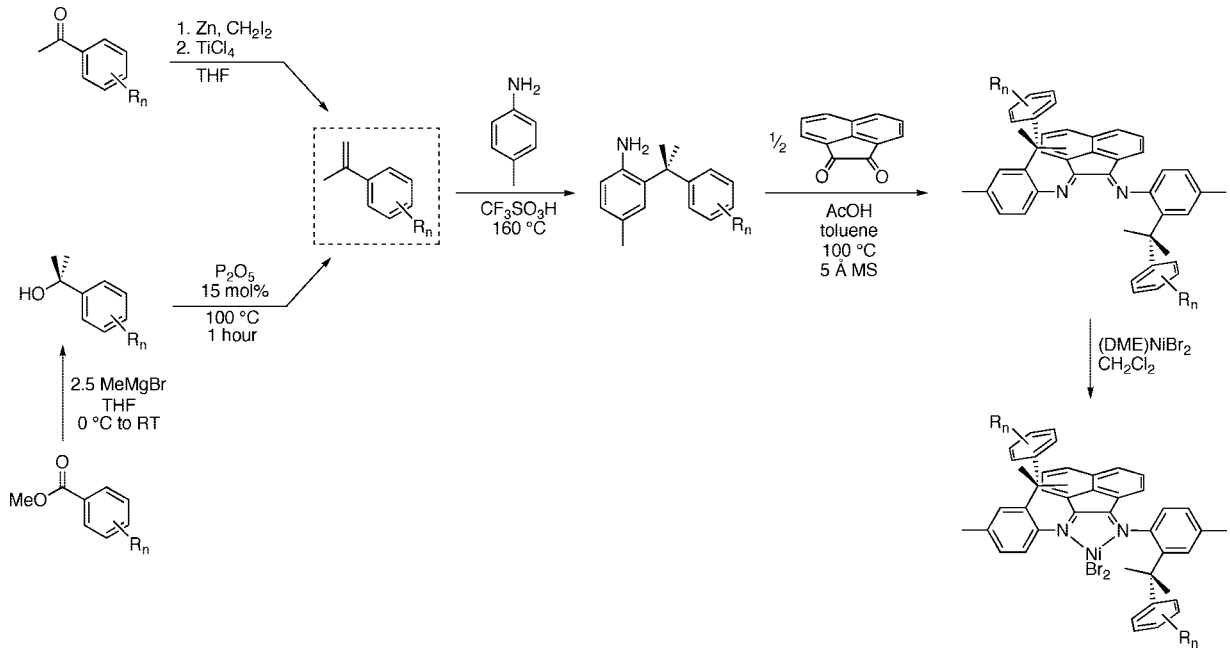

improving the stereoselectivity of the catalyst involves increasing the difference in the steric bulk of the occupied and empty quadrants of the complex. We propose that replacing the hydrogen at each of the two stereocenters with a second methyl group can affect this change. Although this would yield a complex that does not contain stereocenters, the molecule could still retain axial chirality.

The synthesis of these new complexes featuring substituted cumyl groups is depicted in Scheme 2. The methodology again focuses on the acid-catalyzed ortho-alkylation of anilines with styrenes; however, α-methylstyrene derivatives are now employed to yield the desired substituents. In comparison to styrenes, there are far fewer commercially available α-methylstyrenes. Because of this, routes to α-methylstyrenes from both acetophenone and methyl benzoate derivatives are used as a wide variety of these compounds is commercially available. In one route, titanium-mediated olefination is used to convert an acetophenone derivative to the desired α-methylstyrene.[25] In a second route, methyl Grignard addition to a methyl benzoate derivate yields a tertiary alcohol which is then dehydrated using catalytic P_2O_5 to form the desired α-methylstyrene. Reaction of an α-methylstyrene derivative with *p*-toluidine using catalytic CF_3SO_3H yields the desired aniline derivative. The conditions used to form the constituent ligand of *rac*-**1**, which rely on the precipitation of the product from acetic acid, do not work for the cumyl-based ligands. Instead, most preferably, the reaction between a given aniline and acenaphthenequinone is carried out in toluene in the presence of molecular sieves and a catalytic amount of acetic acid. The crude product, which typically contains a portion of monosubstituted dione, is purified either by crystallization or by column chromatography. Metallation involves reaction of the α-diimine ligand with $(DME)NiBr_2$ to yield the desired complex which is purified through crystallization.

Figure 1 provides the series of complexes that have been synthesized. The general structure is drawn with C_2-symmetry as X-ray crystal structures of *rac*-**1**, *rac*-**2**, and *rac*-**7** show C_2-symmetry in the solid state and all of the activated complexes produce highly isotactic polypropylene at low temperature, presumably via an enantiomorphic site-control mechanism that exploits a C_2-symmetric site (vide infra).

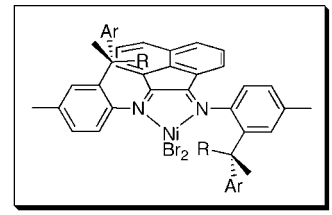

	rac-**1**	*rac*-**2**	*rac*-**3**	*rac*-**4**	*rac*-**5**	*rac*-**6**	*rac*-**7**
R	H	Me	Me	Me	Me	Me	Me
Ar	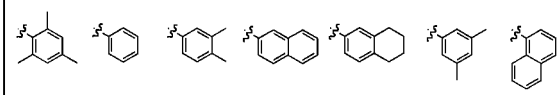						

Figure 1. Ni(II) α-diimine complexes featuring *o*-cumyl-derived aniline moieties.

The ^1H NMR spectra of the constituent diimine ligands of each of the complexes exhibit broad resonances for the aryl and alkyl protons of the aryl substituent off of the *N*-aryl ring. This broadening is more extensive with the constituent ligand of *rac*-**7**; a majority of the resonances in the ^1H NMR spectrum are present as very broad singlets. This phenomenon is likely due to a fluxional $\pi-\pi$ stacking interaction between the acenaphthene backbone and the aryl substituents in each compound. Attaining a ^1H NMR spectrum of the constituent ligand of *rac*-**7** in $CDCl_3$ at 60 °C resulted in a significant sharpening of the peaks.

The X-ray crystal structures of *rac*-**1**,[6] *rac*-**2**, and *rac*-**7** are provided in Figure 2. Each complex is C_2-symmetric in the solid state, and *rac*-**1** and *rac*-**2** are crystallographically C_2-symmetric. The obvious difference between the complex based on a chiral aniline (*rac*-**1**) and the complexes featuring cumyl-type substituents (*rac*-**2** and *rac*-**7**) is the presence of a second methyl group that protrudes toward the center of the molecule. A difference in the dihedral angles about Ni (ϕ between the N−Ni−N and Br−Ni−Br planes) for the two types of complex can also be clearly seen: for *rac*-**1**, $\phi = 65.7$ °, for *rac*-**2**, $\phi = 52.8$ °, and for *rac*-**7**, $\phi = 53.4$ °.

Screening for Propylene Polymerization Behavior. The primary goal of this work is to furnish complexes that exhibit

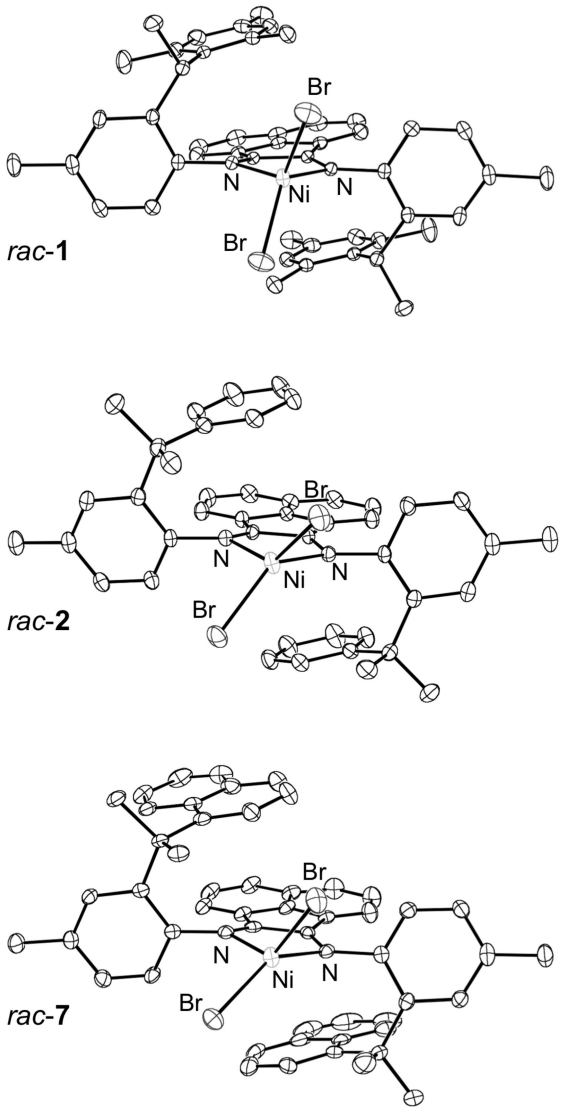

Figure 2. ORTEP diagrams of *rac*-**1**, *rac*-**2**, and *rac*-**7** (molecules of crystallization omitted). Hydrogen atoms are omitted for clarity, and ellipsoids are drawn at the 40% probability level.

the fundamental behaviors of *rac*-**1**/MAO (isoselectivity, temperature-dependent regioselectivity, and livingness) but that offer greater levels of selectivity and higher activity. With this in mind, screening has been primarily focused to propylene polymerization at three relevant temperatures: 0, −60, and −78 °C. Each of the new complexes (*rac*-**2**−*rac*-**7**), upon activation, is in fact isoselective and exhibits temperature-dependent regioselectivity for propylene polymerization; therefore, all screening results are directly compared to *rac*-**1**/MAO.

A summary of 0 °C propylene polymerization screening results for *rac*-**1**−*rac*-**7**/MAO is provided in Table 1. A range of activities is observed for the series with several complexes exhibiting the same or greater activity than *rac*-**1**/MAO. The living behavior of the catalysts under these conditions can be rudimentarily assessed by examining the polydispersity indices (M_w/M_n) of the resultant polymers. In all cases, M_w/M_n is higher than for the polymer produced using *rac*-**1**/MAO with *rac*-**2**/MAO and *rac*-**4**/MAO producing polymers with polydispersity indices ($M_w/M_n \sim 1.5$) outside of the range generally accepted for living polymerization and *rac*-**6**/MAO producing a polymer with a bimodal molecular weight distribution.

The global structure of the polypropylenes produced at 0 °C has also been studied. The mole percent of 3,1-enchainment is quantified using ^{1}H NMR spectroscopy. Not surprisingly, there

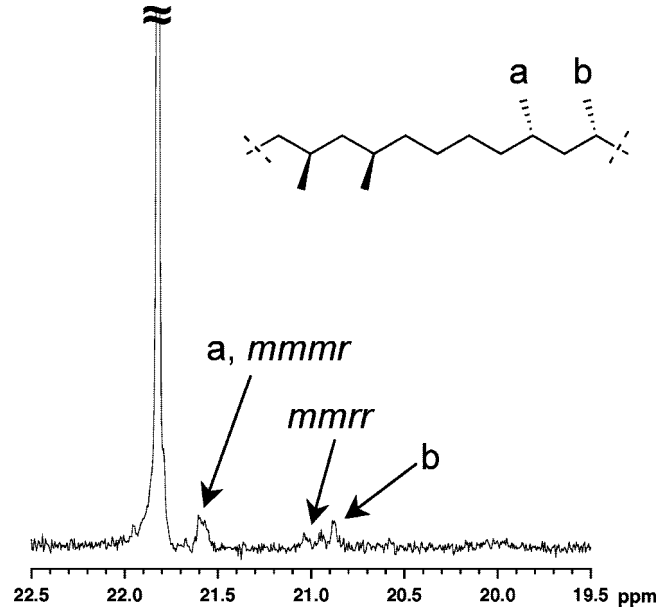

Figure 3. Methyl region of the ^{13}C NMR spectrum (1,1,2,2-$C_2D_2Cl_4$, 125 MHz, 135 °C) of isotactic polypropylene synthesized using *rac*-**7**/MAO at −60 °C (Table 2, entry 6).

is a fairly good correlation between the portion of 3,1-insertion and the glass transition temperature (T_g) of the polymers with a decrease in T_g tracking with an increase in the portion of 3,1-insertion (regioirregularity). The T_g of these polymers is an important parameter vis-à-vis their role as soft blocks in the aforementioned regioblock polypropylenes as it represents the lowest possible temperature at which such a block copolymer can exhibit elastomeric behavior.[26] All polypropylenes produced at 0 °C were amorphous.

A summary of −60 °C propylene polymerization screening results for *rac*-**1**−*rac*-**7**/MAO is provided in Table 2. All of the catalysts screened exhibited a significantly higher activity than that of *rac*-**1**/MAO. Most of the polymers have good agreement between M_n and M_n^{theo} (the theoretical M_n based on the assumption that each metal center produces one polymer chain) and have polydispersity indices (PDIs) similar to that of the polypropylene from *rac*-**1**/MAO. In all cases, the PDIs are somewhat broad ($M_w/M_n \sim 1.3-1.5$); this is likely due to precipitation of the semicrystalline polymer from the reaction mixture at the low reaction temperature employed. Upon activation, complexes *rac*-**2**−*rac*-**7** produced polypropylenes with higher melting points than *rac*-**1** ($T_m = 130$ °C) with *rac*-**7**/MAO yielding a polymer with $T_m = 138$ °C.

Figure 3 depicts the methyl region of the ^{13}C NMR spectrum of the isotactic polypropylene produced at −60 °C using *rac*-**7**/MAO. Small, overlapping peaks present in the baseline correspond to both regioerrors[6,27] and stereoerrors.[28] Analogous with studies conducted using *rac*-**1**/MAO,[6] microstructural errors at low polymerization temperatures consist of isolated 3,1-insertions and stereoerrors expected for a site-control mechanism of stereocontrol.

Selected catalysts were also screened for propylene polymerization behavior at −78 °C; these data are presented in Table 3. Each of the three screened cumyl-based complexes exhibited a 3-fold enhancement in activity over *rac*-**1**/MAO and good agreement between M_n and M_n^{theo}, and PDIs consistent with that of *rac*-**1**/MAO were also established. The melting points of the polypropylenes produced using *rac*-**2**/MAO, *rac*-**3**/MAO, and *rac*-**7**/MAO were higher than for the polypropylene produced using *rac*-**1**/MAO with *rac*-**7**/MAO yielding polypropylene with $T_m = 149$ °C.

Table 1. Propylene Polymerization Screening of *rac*-1−*rac*-7/MAO at 0 °C[a]

entry	cplx	cplx loading (μmol)	yield (mg)	TOF (h^{-1})[b]	M_n^{theo} (kg/mol)[c]	M_n (kg/mol)[d]	M_w/M_n[d]	mol % 3,1 insert.[e]	T_g (°C)[f]
1	*rac*-**1**	17	586	410	34.5	45.4	1.07	31.6	−54
2	*rac*-**2**	17	903	632	53.1	89.9	1.44	22.1	−46
3	*rac*-**3**	17	1490	1043	87.6	149.1	1.26	26.5	−47
4	*rac*-**4**	17	209	146	12.3	56.5	1.45	29.7	−50
5	*rac*-**5**	10	959	1140	95.9	152.4	1.24	18.8	−42
6	*rac*-**6**	17	104	73	6.1	bimodal	bimodal	32.4	−48
7	*rac*-**7**	17	596	417	35.1	134.5	1.17	16.7	−40

[a] 5.0 ± 0.6 g of propylene, 25 mL of toluene, 270 equiv of MMAO-7; t_{rxn} = 2 h. [b] Turnover frequency (TOF) = mol propylene/(mol Ni·h). [c] Determined by the equation: (g polymer)/(mol Ni). [d] Determined by gel permeation chromatography at 140 °C in 1,2,4-trichlorobenzene vs polyethylene standards. [e] Determined by the equation $\chi_{3,1} = [(1 - R)/(1 + 2R)]$, where $R = [CH_3]/[CH_2]$, determined by ^{1}H NMR spectroscopy. [f] Determined by differential scanning calorimetry, second heat.

Table 2. Screening of Select Complexes for Propylene Polymerization at −60 °C[a]

entry	cplx	cplx loading (μmol)	yield (mg)	TOF (h^{-1})[b]	M_n^{theo} (kg/mol)[c]	M_n (kg/mol)[d]	M_w/M_n[d]	mol % 3,1 insert.[e]	T_g (°C)[f]	T_m (°C)[f]	ΔH (J/g)[f]
1	*rac*-**1**	17	110	3	6.5	9.0	1.34	7.6	−14	130	48.0
2	*rac*-**2**	17	884	26	52.0	75.1	1.32	0.7	−10	131	26.8
3	*rac*-**3**	17	1050	31	61.8	64.9	1.45	4.4	−14	132	61.7
4	*rac*-**4**	17	956	28	56.2	72.0	1.39	6.1	−10	129	54.6
5	*rac*-**5**	10	414	20	41.4	54.3	1.26	1.4	−9	135	60.4
6	*rac*-**7**	17	1060	31	62.4	76.4	1.36	3.1	−12	138	47.9

[a] 15.0 ± 0.7 g of propylene, 25 mL of toluene, 270 equiv of MMAO-7; t_{rxn} = 48 h. [b] Turnover frequency (TOF) = mol propylene/(mol Ni·h). [c] Determined by the equation: (g polymer)/(mol Ni). [d] Determined by gel permeation chromatography at 140 °C in 1,2,4-trichlorobenzene vs polyethylene standards. [e] Determined by the equation $\chi_{3,1} = [(1 - R)/(1 + 2R)]$, where $R = [CH_3]/[CH_2]$, determined by ^{1}H NMR spectroscopy. [f] Determined by differential scanning calorimetry, second heat.

Table 3. Screening of Select Complexes for Propylene Polymerization at −78 °C[a]

entry	cplx	yield (mg)	TOF (h^{-1})[b]	M_n^{theo} (kg/mol)[c]	M_n (kg/mol)[d]	M_w/M_n[d]	mol % 3,1 insert.[e]	T_g (°C)[f]	T_m (°C)[f]	ΔH (J/g)[f]
1[g]	*rac*-**1**	73	1	4.3	5.7	1.37	0	−1	137	67
2	*rac*-**2**	108	3	6.4	9.9	1.33	0.7	−11	144	96
3	*rac*-**3**	115	3	6.8	9.8	1.28	0.4	−7	146	90
4	*rac*-**7**	111	3	6.5	9.9	1.36	0	−4	149	104

[a] 15.0 ± 0.5 g of propylene, 25 mL of toluene, 270 equiv of MMAO-7; t_{rxn} = 48 h. [b] Turnover frequency (TOF) = mol propylene/(mol Ni·h). [c] Determined by the equation: (g polymer)/(mol Ni). [d] Determined by gel permeation chromatography at 140 °C in 1,2,4-trichlorobenzene vs polyethylene standards. [e] Determined by the equation $\chi_{3,1} = [(1 - R)/(1 + 2R)]$, where $R = [CH_3]/[CH_2]$, determined by ^{1}H NMR spectroscopy. [f] Determined by differential scanning calorimetry, second heat. [g] t_{rxn} = 96 h.

Summary of Screening Results. Each of the *o*-cumyl catalysts exhibited higher regioselectivity than *rac*-**1**/MAO at low reaction temperatures. This is most evident from the content of 3,1-insertion in polypropylenes produced at −60 °C (Table 2). As for living behavior, the PDIs of the polymers produced at 0 °C using the *o*-cumyl catalysts are higher and the values of M_n and M_n^{theo} are more disparate compared to *rac*-**1**/MAO; the same data for polymers produced at lower temperatures by the cumyl catalysts, though, is more consistent with *rac*-**1**/MAO. Regarding activity, most of the cumyl catalysts exhibited greater activities for propylene polymerization at all temperatures screened compared to *rac*-**1**/MAO. The rate enhancement upon going from *rac*-**1** to the sterically bulkier cumyl complexes is not particularly surprising. Gates et al.[29] showed a dramatic increase in ethylene polymerization activity upon increasing the steric demand about the active site among a series of Ni α-diimine catalysts. The rationale given for the rate enhancement was that increased steric demand about the metal center destabilizes the ground state of monomer insertion relative to the transition state which lowers the barrier to insertion and increases the polymerization activity.[30]

From the screening results, *rac*-**7**/MAO was determined to exhibit the best polymerization behavior in terms of low-temperature activity, livingness, and stereo- and regioselectivity as realized through resultant polypropylene melting temperature. The activity of *rac*-**7**/MAO for propylene polymerization at 0 °C using the standard screening conditions (Table 1) is lower than that of several other catalysts including *rac*-**2**, *rac*-**3**, and *rac*-**5**/MAO. However, when *rac*-**7**/MAO is screened at 0 °C under conditions used for block copolymer synthesis (namely, higher monomer concentration) its activity increases dramatically from 417 h^{-1} to 4700 h^{-1}. In addition, the PDI decreases from 1.17 to 1.08 for the resultant polymer and the agreement between M_n and M_n^{theo} is significantly better. Under the same conditions, *rac*-**1**/MAO exhibits an activity of 1300 h^{-1} and M_w/M_n = 1.10 for the resultant polypropylene. Furthermore, a linear increase in M_n with polymer yield is observed for a series of propylene polymerizations run using *rac*-**7**/MAO at 0 °C (see the Supporting Information).

Synthesis of Regioblock Polypropylenes. Scheme 3 depicts the general strategy for the formation of propylene-based tri- and pentablock copolymers using *rac*-**7**/MAO. Polymerizations are initiated at −60 °C to form an iPP block. After a given amount of time, t_1, the reaction is transferred to a 0 °C bath to form a rirPP block over time t_2. A second temperature change back to −60 °C affords a second iPP block over time t_3. Quenching at this point yields a triblock copolymer, whereas subjecting the polymerization to additional temperature changes yields additional blocks.

Table 4 summarizes the characterization data for the regioblock copolymers that were synthesized using *rac*-**7**/MAO. For comparison, previously reported samples synthesized using *rac*-**1**/MAO are also provided (***isoTB*** and ***isoPB***).[23] For **isoTB2** (entry 2), block lengths were chosen to mimic those of ***isoTB*** (entry 1) so as to provide a direct comparison between *rac*-**1** and *rac*-**7**. As expected, **isoTB2** exhibits a higher melting point than ***isoTB*** and because *rac*-**7**/MAO is more regioselective than *rac*-**1**/MAO at 0 °C, the estimated fraction of ethylene (F_e) in the soft block of the polymer is estimated to be only 0.24 for **isoTB2** compared to 0.53 for ***isoTB***. This difference is manifested as a difference in T_g (−35 °C for **isoTB2** vs −44 °C for ***isoTB***). Other triblock copolymer samples with lower hard block contents were synthesized; **isoTB3** and **isoTB4**

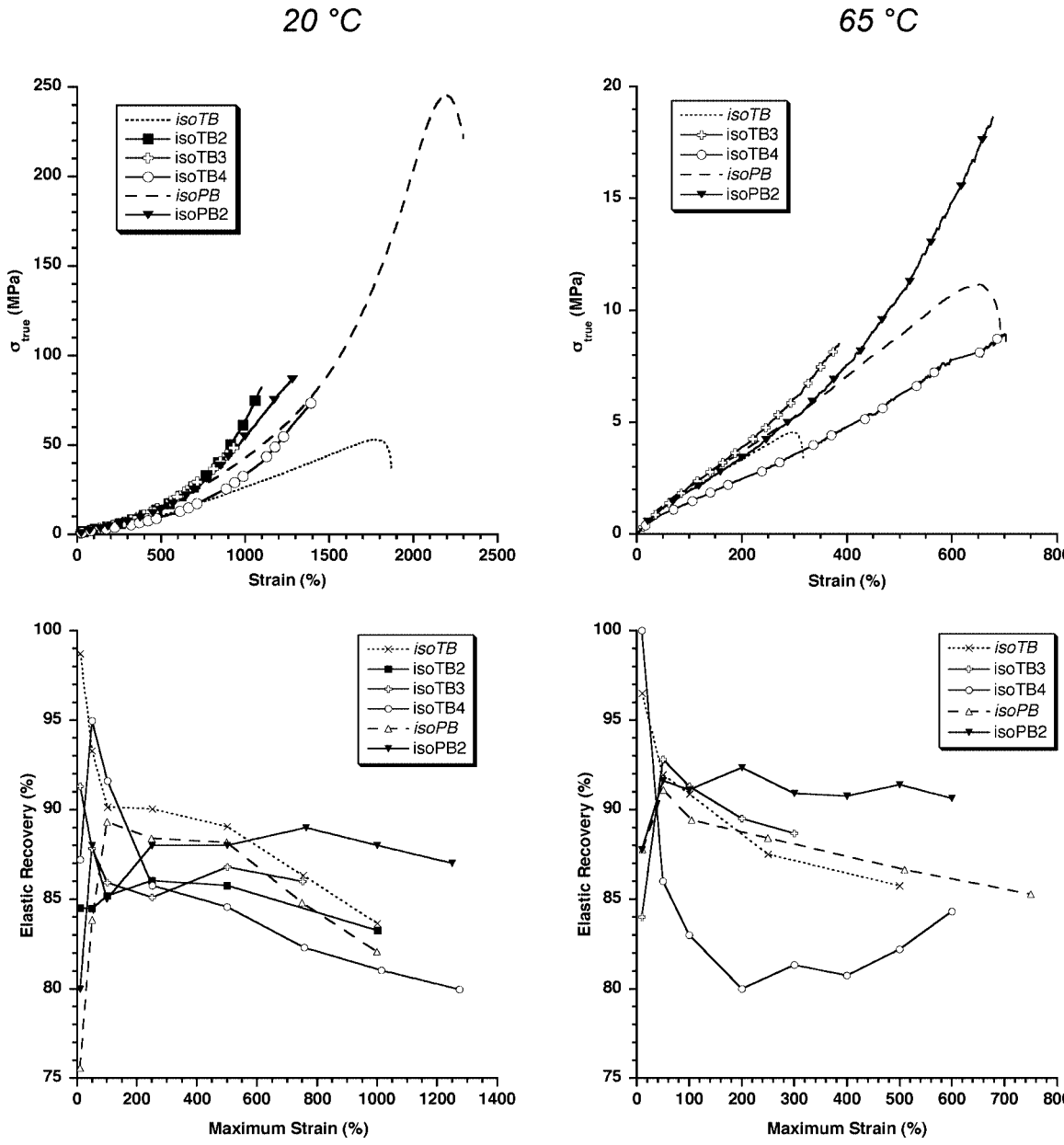

Figure 4. Plots of tensile true stress vs percent strain (top) and elastic recovery vs maximum strain (bottom) at 20 °C (left) and 65 °C (right) for the tri- and pentablock copolymers (Table 4).

Scheme 3. Synthesis of Propylene-Based Tri- And Pentablock Copolymers Using *rac*-7/MAO

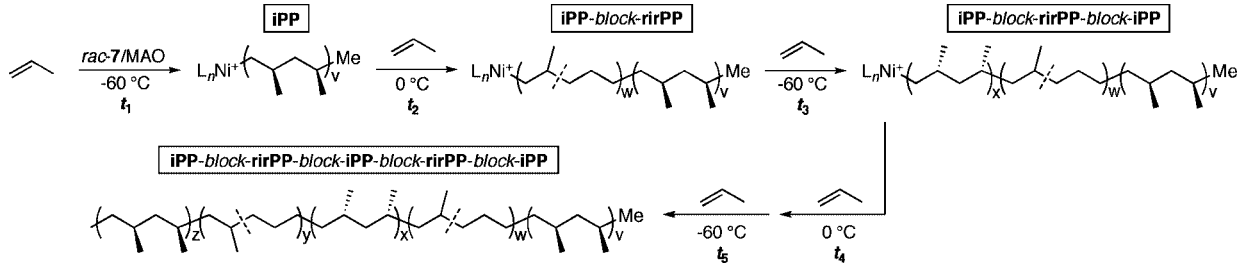

contain 19 and 17 wt % hard blocks, respectively. In addition, a pentablock copolymer with approximately the same composition of hard blocks as ***isoPB*** has been synthesized (**isoPB2**, entry 6). The higher activity of *rac*-**7**/MAO compared to that of *rac*-**1**/MAO has led to a 70−80% reduction in the total reaction time required for the synthesis of the block copolymers (t_{rxn}^{tot}); for **isoTB2**, $t_{rxn}^{tot} = 24$ h compared to 118 h for ***isoTB*** while for **isoPB2**, $t_{rxn}^{tot} = 50$ h compared to 166 h for ***isoPB***.

Mechanical Testing. Stress−strain curves and plots of elastic recovery as a function of maximum strain for the tri- and pentablock copolymers are presented in Figure 4 (legend entries for samples synthesized using the original catalyst, *rac*-**1**/MAO, are in italics). Measurements were made at both room temperature (~20 °C) and 65 °C for a majority of the samples. Table 5 summarizes the mechanical testing results at both temperatures.

Table 4. Block Copolymer Characterization Summary

entry	sample	cplx used	M_n, tot (kg/mol)[a]	M_w/M_n[a]	block lengths, M_n (kg/mol)[a]	wt % of hardblocks[b]	estimated F_e in soft blocks[c]	T_g (°C)[d]	T_m (°C)[d]	ΔH (J/g)[d]
1	**isoTB**	*rac*-**1**	109	1.14	10−83−16	24	0.53	−44	129	5.5
2	**isoTB2**	*rac*-**7**	117	1.12	15−86−16	26	0.24	−35	140	13.1
3	**isoTB3**	*rac*-**7**	125	1.17	13−101−10	19	0.24	−35	137	13.4
4	**isoTB4**	*rac*-**7**	163	1.15	20−136−8	17	0.24	−34	137	8.3
5	**isoPB**	*rac*-**1**	159	1.39	16−75−6−46−16	24	0.53	−46	125	9.5
6	**isoPB2**	*rac*-**7**	199	1.22	15−89−14−63−17	23	0.24	−39	134	9.3

[a] Determined using GPC in 1,2,4-$C_6H_3Cl_3$ at 140 °C vs polyethylene standards. [b] Wt % of hard blocks = $(\sum M_{n,hard})/(M_{n,tot})$. [c] Mole fraction of ethylene (F_e) in rirPP block(s) determined by the equation: $F_e = 1.5(\%\ 3,1\text{-insertions})/[(100 - \%\ 3,1\text{-insertions}) + 1.5(\%\ 3,1\text{-insertions})]$, where % 3,1-insertions = $[(1 - R)/(1 + 2R)] - 100$, and $R = [CH_3]/[CH_2]$, determined by ^{1}H NMR. [d] Determined by differential scanning calorimetry, second heat.

Table 5. Summary of Mechanical Testing for the Tri- And Pentablock Copolymers of Table 4

	Young's modulus (MPa)		approximate strain at break (%)		true stress at break (MPa)		elastic recovery (%)[a]	
sample	20 °C	65 °C	20 °C	65 °C	20 °C	65 °C	20 °C	65 °C
isoTB	3.5	2.7	1800	300	53	5	84	86
isoTB2	6.0		1100		82		83	
isoTB3	3.8	2.6	1000	390	50	9	86	89
isoTB4	3.0	2.2	1400	700	74	9	80	84
isoPB	3.5	2.7	2200	650	245	11	82	85
isoPB2	3.9	2.8	1300	680	88	19	87	91

[a] Measured after the last step-strain cycle before fracture.

From the data obtained at 20 °C, two of the triblock copolymers synthesized using *rac*-**7**/MAO (**isoTB2** and **isoTB4**) exhibited a higher true stress at break than ***isoTB***, albeit at a lower strain. Of all the samples synthesized using *rac*-**7**/MAO, **isoPB2** exhibited the highest true stress at break (88 MPa) and strain at break (∼1300%) although these values fall far short of those for ***isoPB*** which exhibited a true stress at break of 245 MPa and a strain at break of ∼2200%. Although this result is disappointing, the soft blocks of the polymers synthesized using *rac*-**7**/MAO have a significantly lower fraction of ethylene than those of ***isoTB*** and ***isoPB*** (0.24 vs 0.53). This relatively low ethylene content could impart miscibility between the hard and soft blocks that would be expected to diminish elastomeric performance. Elastic recoveries for the triblocks synthesized using *rac*-**7**/MAO are similar to those of ***isoTB*** with **isoTB3** exhibiting a marginally higher percent elastic recovery (86%) than ***isoTB*** (84%). A more significant increase is observed for **isoPB2** versus ***isoPB*** with elastic recovery values of 87% versus 82%, respectively.

At 65 °C, most of the block copolymers synthesized using *rac*-**7**/MAO outperformed their *rac*-**1**/MAO analogues. For example, **isoTB4** exhibited a maximum true stress of 9 MPa (compared to 5 MPa for ***isoTB***) and maximum strain of ∼700% (compared to ∼300% for ***isoTB***). Moreover, in the case of **isoTB4** (as well as **isoTB3** and **isoPB2**) these maximal true stresses and strains represent lower limits since, in all cases, the tests terminated when the elastomer slipped from the grips. However, **isoTB4** exhibits slightly inferior elastic recovery compared to ***isoTB*** (84% vs 86%), probably due to its very asymmetric end block lengths. The pentablock copolymer made using *rac*-**7**/MAO, **isoPB2**, significantly outperformed ***isoPB*** exhibiting a maximum true stress of 19 MPa with a maximum strain of ∼680%. Sample **isoPB2** also exhibited better elastic recovery than ***isoPB*** at 65 °C (91% vs 85%). The better performance exhibited at 65 °C for the block copolymers synthesized using *rac*-**7**/MAO is likely due to the higher melting point and heat of fusion of these polymers relative to those of ***isoTB*** and ***isoPB***. As previously proposed,[23] the temperature at which the hard segments of the block copolymers can begin to pull out from the iPP crystallites that are present in the regioirregular polypropylene matrix should be proportional to the melting temperature and heat of fusion of the polymer.

At room temperature, with the exception of **isoTB4**, the Young's modulus of each of the samples synthesized using *rac*-**7**/MAO are higher than their *rac*-**1** analogues. This may be due to the increase in the T_g of the amorphous phase (from about −45 to about −35 °C) as a result of a decrease in the mole fraction of ethylene in the soft blocks. Within the series of materials prepared using *rac*-**7**/MAO, Young's modulus increases as the hard block content and, thus, overall crystallinity increases. At 65 °C, all samples have a lower Young's modulus than at room temperature, probably as a consequence of the decrease of the modulus of the amorphous phase. With the exception of **isoTB4** again, all samples have approximately the same Young's modulus. This result may be explained by the fact that the elastic modulus becomes less sensitive to the T_g of the soft phase as the temperature is increased to well above T_g.

The increased isoselectivity of *rac*-**7**/MAO affords iPP-based hard blocks with higher melting temperatures and heat of fusion values, compared to those synthesized using *rac*-**1**/MAO; this difference is likely the reason for enhanced elastomeric behavior at 65 °C. However, *rac*-**7**/MAO also forms polypropylene that is more regioregular (i.e., more PP-like) than *rac*-**1**/MAO at 0 °C which is likely the cause of the generally inferior elastomeric behavior for **isoTB2**−**isoTB4** and **isoPB2** at 20 °C. Although increasing the polymerization temperature should afford more regioirregular (and less iPP miscible) soft blocks, living behavior begins to diminish at reaction temperatures approaching 25 °C as evidenced by a significant increase in PDI values for the resultant polymers. Further development may be necessary to furnish a catalyst whose temperature range can be extended such that sufficiently ethylene-rich regioirregular polypropylene can be formed in a living fashion.

Conclusions

In an attempt to improve upon the propylene polymerization behavior of a previously reported chiral, C_2-symmetric Ni α-diimine catalyst (*rac*-**1**/MAO), a series of new chiral complexes based on cumyl-derived aniline moieties was synthesized. Screening results for propylene polymerization revealed that each of the new complexes exhibited similar behavior to *rac*-**1**/MAO producing isotactic polypropylene at low reaction temperatures and regioirregular polypropylene at elevated temperatures. In general, the new catalysts were more active than *rac*-**1**/MAO and produced isotactic polypropylene with higher melting temperatures.

A complex featuring 1-naphthyl substituents off of the *N*-aryl rings (*rac*-**7**) was deemed to be the best of the new series and

was taken on to synthesize new elastomeric regioblock polypropylenes featuring three and five blocks. Mechanical testing results revealed that these new polymers exhibit inferior elastomeric behavior to analogous polymers made using the original catalyst at 20 °C. However, at 65 °C, the new polymers generally outperform the original materials in terms of true stress at break and elastic recovery.

Acknowledgment. The authors gratefully acknowledge Professor Glenn H. Fredrickson for invaluable insight and helpful discussion. G.W.C. gratefully acknowledges support from Mitsubishi Chemicals. This material is based upon work supported in part by the U.S. Army Research Laboratory and the U.S. Army Research Office under Grant No. DAAD19-02-1-0275 MAP MURI. This research made use of the Cornell Center for Materials Research Shared Experimental Facilities supported through the NSF MRSEC program (DMR-0520404) and the UCSB Materials Research Laboratory Central Facilities supported through the NSF MRSEC program (DMR-0520415).

Supporting Information Available: Experimental procedures for the synthesis of the complexes, a plot of M_n versus conversion for propylene polymerization using *rac*-**7**/MAO, and crystal data and structure refinement parameters. This material is available free of charge via the Internet at http://pubs.acs.org.

References and Notes

(1) (a) Coates, G. W.; Hustad, P. D.; Reinartz, S. *Angew. Chem., Int. Ed.* **2002**, *41*, 2236–2257. (b) Domski, G. J.; Rose, J. M.; Coates, G. W.; Bolig, A. D.; Brookhart, M. *Prog. Polym. Sci.* **2007**, *32*, 30–92.
(2) Ittel, S. D.; Johnson, L. K.; Brookhart, M. *Chem. Rev.* **2000**, *100*, 1169–1203.
(3) Johnson, L. K.; Killian, C. M.; Brookhart, M. *J. Am. Chem. Soc.* **1995**, *117*, 6414–6415.
(4) Pellecchia, C.; Zambelli, A.; Oliva, L.; Pappalardo, D. *Macromolecules* **1996**, *29*, 6990–6993.
(5) Cherian, A. E.; Lobkovsky, E. B.; Coates, G. W. *Chem. Commun.* **2003**, 2566–2567.
(6) Cherian, A. E.; Rose, J. M.; Lobkovsky, E. B.; Coates, G. W. *J. Am. Chem. Soc.* **2005**, *127*, 13770–13771.
(7) Killian, C. M.; Tempel, D. J.; Johnson, L. K.; Brookhart, M. *J. Am. Chem. Soc.* **1996**, *118*, 11664–11665.
(8) Gottfried, A. C.; Brookhart, M. *Macromolecules* **2001**, *34*, 1140–1142.
(9) Schmid, M.; Eberhardt, R.; Klinga, M.; Leskela, M.; Rieger, B. *Organometallics* **2001**, *20*, 2321–2330.
(10) Gottfried, A. C.; Brookhart, M. *Macromolecules* **2003**, *36*, 3085–3100.
(11) Hicks, F. A.; Jenkins, J. C.; Brookhart, M. *Organometallics* **2003**, *22*, 3533–3545.
(12) Camacho, D. H.; Guan, Z. *Macromolecules* **2005**, *38*, 2544–2546.
(13) Rose, J. M.; Cherian, A. E.; Coates, G. W. *J. Am. Chem. Soc.* **2006**, *128*, 4186–4187.
(14) Johnson, L. K.; Mecking, S.; Brookhart, M. *J. Am. Chem. Soc.* **1996**, *118*, 267–268.
(15) Younkin, T. R.; Conner, E. F.; Henderson, J. I.; Friedrich, S. K.; Grubbs, R. H.; Bansleben, D. A. *Science* **2000**, *287*, 460–462.
(16) Chen, G.; Ma, X. S.; Guan, Z. *J. Am. Chem. Soc.* **2003**, *125*, 6697–6704.
(17) Li, X. F.; Li, Y. G.; Li, Y. S.; Chen, Y. X.; Hu, N. H. *Organometallics* **2005**, *24*, 2502–2510.
(18) Luo, S.; Jordan, R. F. *J. Am. Chem. Soc.* **2006**, *128*, 12072–12073.
(19) Popeney, C. S.; Camacho, D. H.; Guan, Z. *J. Am. Chem. Soc.* **2007**, *129*, 10062–10063.
(20) Guan, Z.; Cotts, P. M.; McCord, E. F.; McLain, S. J. *Science* **1999**, *283*, 2059–2062.
(21) Guan, Z. *J. Polym. Sci., Part A: Polym. Chem.* **2003**, *41*, 3680–3692.
(22) Rose, J. M.; Cherian, A. E.; Lee, J. H.; Archer, L. A.; Coates, G. W.; Fetters, L. J. *Macromolecules* **2007**, *40*, 6807–6813.
(23) Hotta, A.; Cochran, E.; Ruokolainen, J.; Khanna, V.; Fredrickson, G. H.; Kramer, E. J.; Shin, Y. W.; Shimizu, F.; Cherian, A. E.; Hustad, P. D.; Rose, J. M.; Coates, G. W *Proc. Natl. Acad. Sci. U.S.A.* **2006**, *103*, 15327–15332.
(24) Cherian, A. E.; Domski, G. J.; Rose, J. M.; Lobkovsky, E. B.; Coates, G. W. *Org. Lett.* **2005**, *7*, 5135–5137.
(25) (a) Lombardo, L. *Tetrahedron Lett.* **1982**, *23*, 4293–4296. (b) Hibino, J.; Okazoe, T.; Takai, K.; Nozaki, H. *Tetrahedron Lett.* **1985**, *26*, 5579–5580.
(26) Shih, C.-K.; Su, A. C. L. In *Thermoplastic Elastomers: A Comprehensive Review*; Legge, N. R., Holden, G., Schroeder, H. E., Eds.; Hanser Publishers: New York, 1987.
(27) Soga, K.; Shiono, T. *Makromol. Chem., Rapid Commun.* **1987**, *8*, 305–310.
(28) Busico, V.; Cipullo, R. *Prog. Polym. Sci.* **2001**, *26*, 443–533.
(29) Gates, D. P.; Svejda, S. A.; Onate, E.; Killian, C. M.; Johnson, L. K.; White, P. S.; Brookhart, M. *Macromolecules* **2000**, *33*, 2320–2334.
(30) Deng, L.; Woo, T. K.; Cavallo, L.; Margl, P. M.; Ziegler, T. *J. Am. Chem. Soc.* **1997**, *119*, 6177–6186.

MA8019943